Photovoltaic Effect of SnS/CdS Heterostructure

A. Voznyi, Yu. Yeromenko, V. Kosyak, I. Shpetnyi, M. Kolesnyk, A. Opanasyuk
Sumy State University, Sumy, Ukraine

I. Iatsunskyi
NanoBioMedical Centre, AMU,
Poznań, Poland
andrey.vozny@gmail.com

***Abstract*— Tin sulphide is a promising absorber material for low-cost and earth abundant thin film solar cells. In this regard, we have studied phase composition, structural, and electrical properties of *n*-CdS/*p*-SnS heterostructure obtained by the close spaced vacuum sublimation (CSS) method. Surface and cross-sectional morphology of the structure were studied by using of field emission scanning electron microscope (FESEM). Thickness of the layers (450 nm for SnS and 550 nm for CdS) and growth mechanism were determined directly from heterostructure cross-section. Crystal structure and films purity were studied by X-ray diffraction (XRD) and Raman spectroscopy methods. The light current density-voltage (*J-V*) characteristic showed small photovoltaic effect with an open-circuit voltage (V_{oc}) of 0.058 mV, a short circuit current density (J_{sc}) of 3.83 mA/cm^2, a fill factor (*FF*) of 0.41 and an efficiency (η) of 0.092 %.**

Keywords —phase composition, thin films;CSS method, SnS; CdS; heterostructure, solar cell

I. Introduction

Nowadays traditional energy sources are limited, therefore interest for renewable energy is rapidly increasing. Among them, the energy of sun is the most environmental friendly and economically available renewable energy source. More than 50 years a mankind have been converting solar energy into electricity, using solar cells based on silicon wafer, silicon ribbon and GaAs technology. Unfortunately, the fabrication technology of such solar cells is expensive and time consuming. Therefore, alternative approaches to the design of novel solar cells have been developed, and the thin film solar converters is one of the possible options. The most promising among thin film structures are solar cells based on the heterojunction using the CdTe, $CuIn(S,Se)_2$ (CIS), $CuIn_xGa_{(1-x)}(S,Se)_2$ (CIGS) absorber layers [1–4]. One of the main point for reducing a cost of solar cells fabrication is a searching for new materials. It is important to find low-cost materials with optimal structural, electrical and optical properties. In particular with a small number of structural defects, with high carrier mobility and long carrier lifetime, with high absorption coefficient and suitable optical band gap.

SnS is considered to be a non-toxic semiconductor material promising for solar cells application. It consists of the low-cost and earth-abundant elements (tin and sulphur). Tin sulphide has an suitable for the strong light absorption band gap (1,1 – 1,5 eV), a high absorption coefficient of $\alpha > 10^4$ cm^{-1} and an intrinsic concentration of charge carriers $[p]\sim10^{15}$ cm^{-3} [5–7]. These properties make it promising material for application as an absorber layer in thin film solar cells [6–7]. Unlike $Cu_2ZnSn(S,Se)_4$ (CZTS) semiconductor, which has been proposed as absorber layer [8], SnS films can be obtained by relatively cheap and technologically simple methods. Usually it can be prepared by using sulphurisation, magnetron sputtering, electrochemical deposition, spray pyrolysis and thermal vacuum evaporation techniques [6].

Traditional buffer layer of thin film solar cells is a cadmium sulphide (CdS). It has wide band gap (2,42 – 2,45 eV), which is close to optimal for high transmittance of light in the visible, and a high reflectance in the infrared spectral region [9]. Conventionally, deposition of typical CdS buffer layer is performing by using of chemical methods, first of all, chemical bath deposition [9].

CSS is a widespread method for fabrication of high-efficiency CdTe based solar cells [10]. This technique allows to obtain high crystal quality and stoichiometric binary semiconductor films under controllable technological process [11–13]. Therefore, in this work SnS and CdS films were deposited by CSS method.

Ref. [14] reports study of solar cells using thermally evaporated SnS and CdS layers. However, formation of *n*-CdS/*p*-SnS heterostructures obtained by CSS method has not yet been studied.

Thus, the goal of this work is to fabricate *n*-CdS/*p*-SnS photovoltaic structure by CSS method and to determine the main solar cell parameters, as well as to study the phase composition and structural properties of CdS and SnS films.

II. Experimental

A. Thin film deposition and heterostructure fabrication

SnS based solar cell was fabricated in superstrate configuration. CdS and SnS films were deposited in a VUP-5M vacuum chamber using CSS method with a vacuum level of $\leq5\times10^{-4}$ Pa. A detailed description of the CSS method is presented in [15]. All layers were obtained using the stoichiometric powders of cadmium sulphide and tin sulphide, respectively. ITO-coated glass substrates were ultrasonically cleaned in the isopropanol for 10 minutes prior to the deposition of CdS film.

CdS film was obtained using the following growth conditions: evaporator temperature of 700 °C, substrate temperature of 450 °C, and deposition time of 3 min. Whereas, SnS absorber layer was deposited on ITO/CdS structure under evaporator temperature of 725 °C, substrate temperature of 250 °C, and deposition time of 2 min. Tin back metal contacts was deposited by vacuum thermal evaporation technique on SnS layer. Contact area is 3.14 mm^2.

Schematic diagram of ITO/CdS/SnS heterostructure are shown in fig. 1.

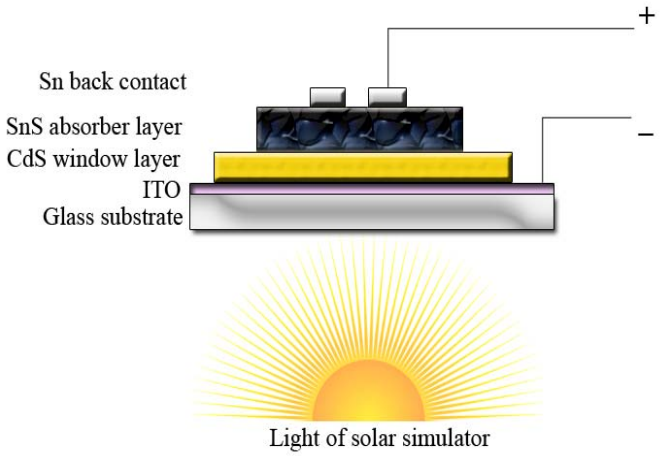

Fig. 1. The schematic diagram of ITO/CdS/SnS heterostructure fabricated in superstrate solar cell configuration

B. Thin films characterization

Surface and cross-sectional morphology of the sample were studied using FEI Nova NanoSEM 650 field emission scanning electron microscope.

The phase composition analysis of the layers was investigated using Rigaku Ultim+ X-ray diffractometer with $K_\alpha Cu$ radiation source. The measurement were carried out in the range from 10° to 80° 2θ angles. The identification of the crystal phases was performed by comparing interplane distances and relative intensities of the lines with reference data for CdS and SnS single crystals (PDF-2 database).

Raman analysis was carried out using micro-Raman spectrometer Renishaw InVia90V727. Room temperature measurements for CdS and SnS films were conducted in the range of 80-2000 cm^{-1}. As the excitation source was used Ar green laser (λ =514 nm). The signals was recorded using CCD camera. Calibration of the micro-Raman spectrometer was carried out by measuring the 520 cm^{-1} Raman line of the silicon. The parameters of measurement was set up to get strong enough signal-to-noise ratio of the spectra.

C. Solar cell characterization

Tektronix 4020 DMM and a stabilised voltage source was used for the light and dark *J-V* measurements of the sample. The light *J-V* characteristics of the solar cell was measured at room temperature under 1.5 AM illumination, using LED-light solar simulator. Such simulator with different light-emitting diodes helps to create light flux with parameters similar to solar radiation.

Light *J-V* curve of ITO/CdS/SnS heterostructure allows to determine basic solar cell parameters (V_{oc}, J_{sc}, *FF*, and η).

FF was calculated via the equation:

$$FF = \frac{P_{\max}}{I_{sc} V_{oc}}, \quad (1)$$

where $P_{\max}$ –output maximum power of solar cell.

J_{sc} was calculated using the following expression:

$$J_{sc} = I_{sc} / S, \quad (2)$$

where *S* is area of the contact.

Photovoltaic efficiency of *n*-CdS/*p*-SnS solar cell was calculated from the well-known formula:

$$\eta = \frac{I_{sc} V_{oc} FF}{P_{in}}, \quad (3)$$

where P_{in} is the input power of light illumination (P_{in} = 100 mW/cm^2.

III. RESULTS

Fig. 2 shows FESEM images of the surface morphology of SnS film (a) and cross-sectional image of ITO/CdS/SnS structure (b). As can be seen from Fig. 2 (a), SnS film consists of randomly oriented blade-like crystallites with an average size and thickness of 300 and 20 nm, respectively.

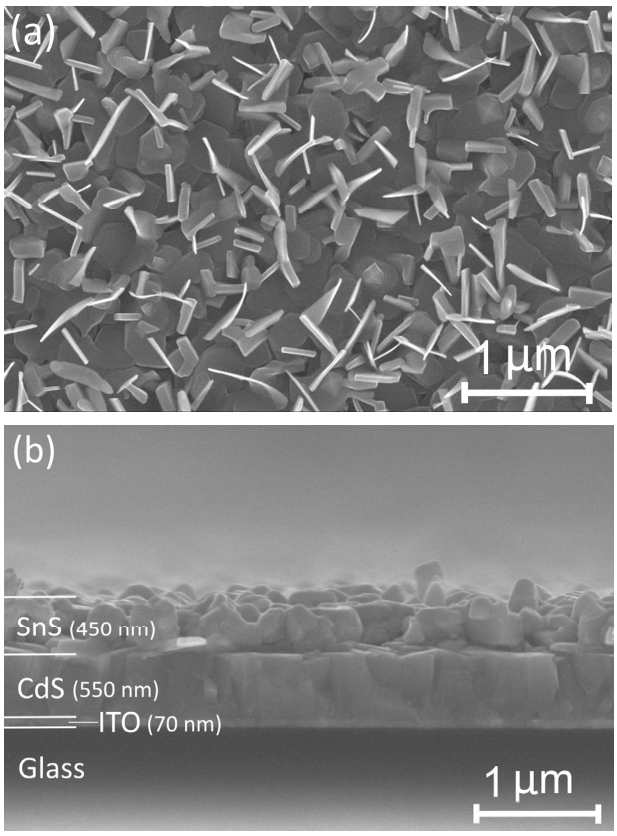

Fig. 2. Plane-view FESEM image of SnS film (a) and cross-sectional image of ITO/CdS/SnS structure (b)

Cross-sectional analysis of ITO/CdS/SnS structure (Fig. 2 (b)) allowed to estimate the average layer thicknesses and to determine their growth mechanism. Hereby, heterostructure consists of ITO transparent conductive layer (70 nm), CdS buffer layer (550 nm), and SnS absorber layer (450 nm). It

was found that CdS and SnS films have a columnar crystal structure which is preferable for highly effective solar cell. Due to the high absorption coefficient (10^4 cm^{-1}) of SnS [16–17] 450 nm film thickness can provide sufficient absorption of the incident sunlight. For example, the record solar cell with an efficiency of 4.4% contained 500 nm thick of SnS film [18]. It should also be noted that films have no voids, pores and cracks, which presence adversely affected on the electrical parameters of the solar cells.

To avoid misinterpretation of the phase composition analisys of ITO/CdS/SnS heterostructure, which may be associated with peaks overlapping of different phases on XRD patterns, the measurements were carried out in the following steps: 1) ITO-coated glass substrate was measured; 2) measurement of ITO/CdS structure was performed; 3) ITO/CdS/SnS heterostructure was studied.

XRD analysis of ITO layer (Fig. 3(a), black line) reveals reflection from the (222), (400) and (441) crystallographic planes of the cubic phase of $In_2Sn_2O_{7-x}$ (PDF-2 card № 00-039-1058). XRD pattern of ITO/CdS two-layer structure (Fig. 3(b), green line) shows strong intense peaks from the (002), (004), (105) and weak intense peaks from the (100), (103), (112) planes that in good agreement with the hexagonal phase (wurtzite) of CdS (PDF-2 card № 00-041-1049). It should be noted that no reflections from the crystallographic planes of the cubic phase (sphalerite) of CdS, which could also be formed in the films [19], were detected.

XRD pattern of ITO/CdS/SnS heterostructure are shown in Fig. 3(c), blue line. In addition to the peaks of ITO and CdS, reflections from the (101), (040), (131), (212), (251) and (171) crystallographic planes of the orthorhombic SnS phase were detected (PDF-2 card № 00-014-0620). Furthermore, a very weak peak from the (260) plane of the orthorhombic Sn_2S_3 phase was found (PDF-2 card № 00-030-1379).

To study the vibrational properties and phase composition of the films the Raman analysis was carried out. It is well known that this method is a good complement to the XRD analysis in the case of the presence of secondary phases in material.

Fig. 4 shows Raman spectra of CdS (a) and SnS (b) films. Raman spectrum of CdS film exhibits a clear intense peak at 301 cm^{-1} that corresponds to the longitudinal optical phonon (1LO) mode and its overtone (2LO) at 603.2 cm^{-1} [20]. According to Ref. [21], the frequencies of the cubic wurtzite structure coincide with the frequencies of the hexagonal sphalerite structure of CdS, and hence cannot be used to identify these two structures.

As can be seen from Fig. 4(b), Raman spectra exhibits SnS-related lines at 92.8, 185.6, 221.6 and 288.6 cm^{-1} of A_g vibrational mode. Along with this, B_{2g} mode at 158 cm^{-1} of SnS was observed. Weak peak at 307.8 cm^{-1} that corresponds to A_g mode of sulfur-rich Sn_2S_3 phase was also detected.

Thus, based on XRD and Raman spectroscopy data CdS layer is single-phase with hexagonal wurtzite crystal structure, while the SnS layer is predominantly single-phase with a small amount of Sn_2S_3 secondary phase.

Fig. 4 shows dark and light (in the inset) *J-V* characteristics of *n*-CdS/*p*-SnS heterojunction. Dark *J-V* curve has a typical diode behaviour. The rectification factor of 200 was calculated as the ratio of currents at -0.5 and +0.5 V.

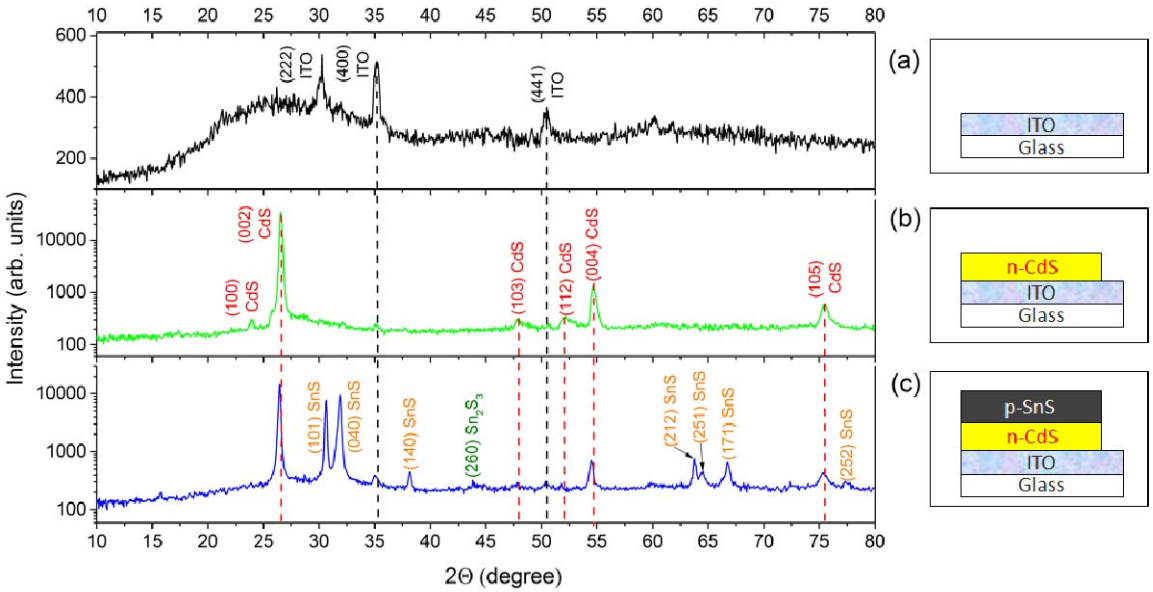

Fig. 3. XRD data of ITO ((a), black line), ITO/CdS ((b), green line) and ITO/CdS/SnS ((c), blue line)

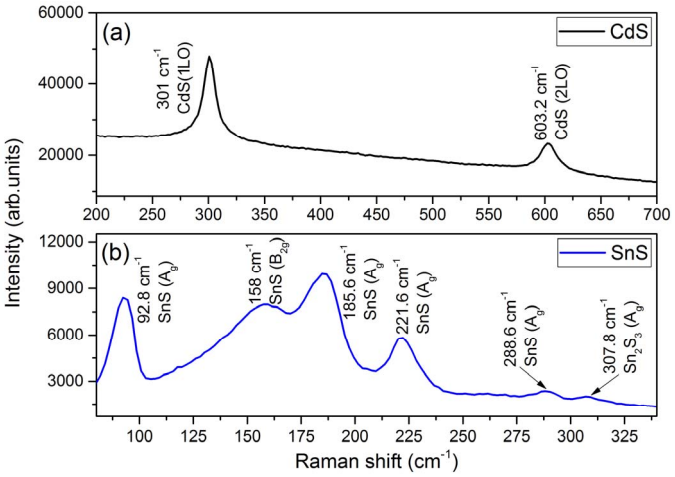

Fig. 4 Ramans spectra of CdS (a) and SnS (b) films

The main parameters of solar cell were determined from the light *J-V* curve (Fig. 4, insert): V_{oc} is 0.058 V, J_{sc} is 3.38 mA/cm^2, *FF* is 0.41, and η is 0.092%. These parameters are significantly lower than those of the record SnS solar cell [18].

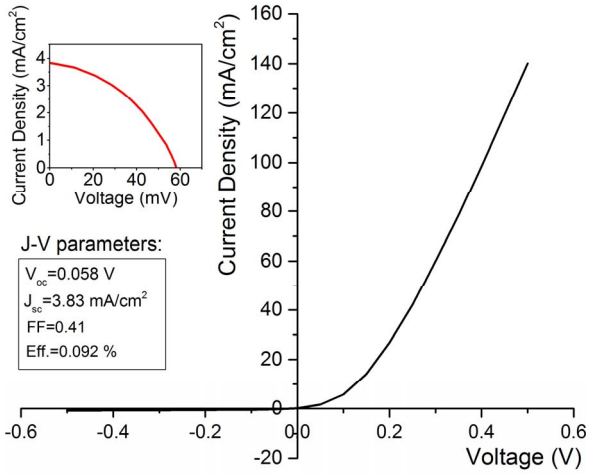

Fig.4. Dark and light (in the inset) *J-V* characteristics of *n*-CdS/*p*-SnS heterojunction

The low V_{oc} value may be explained by the unfavorable band alignment of SnS with conventional CdS buffer layer [22]. Small J_{sc} value and consequently, poor solar cell efficiency may be associated with minority carriers recombination at the grain boundaries, defects [6], [18] and too large thickness of CdS buffer layer.

IV. Conclusions

We have studied the structural and electrical properties as well as phase composition of *n*-CdS/*p*-SnS heterojunction obtained by the CSS method. It was found that the layers of solar cell have columnar crystal structure with 550 and 450 nm thick for CdS and SnS, respectively. SnS film consists of blade-like crystallites with an average size of 300 nm and 20 nm thick. CdS layer has single-phase hexagonal (wurtzite) crystal structure, while the SnS layer has predominantly single-phase structure with a small amount of Sn_2S_3 phase. Dark *J-V* curve of *n*-CdS/*p*-SnS heterojunction has a typical diode behavior with a rectification factor of 200 as the ratio of currents at -0.5 and +0.5 V was observed. Under illumination, photovoltaic effect with V_{oc} of 0.058 V, J_{sc} of 3.38 mA/cm^2, *FF* of 0.41 and η of 0.095% was observed.

Acknowledgments

This work was supported by the Ministry of Education and Science of Ukraine (Grants №0116U002619, №0115U000665c and №0116U006813)

References

[1] R. Scheer and W. Schock, Chalcogenide Photovoltaics: physics, technologies, and thin film devices. WILEY–VCH Verlag GmbH & Co. KGaA, 2011.

[2] G. S. Khrypunov, E. P. Chernykh, N. A. Kovtun, and E. K. Belonogov, "Flexible solar cells based on cadmium sulfide and telluride," Semiconductors, vol. 43, no. 8, pp. 1046–1051, 2009..

[3] N. P. Klochko, G. S. Khrypunov, N. D. Volkova, V. R. Kopach, A. V Momotenko, and V. N. Lyubov, "Structure and properties of electrodeposited films and film stacks for precursors of chalcopyrite and kesterite solar cells," Semiconductors, vol. 48, no. 4, pp. 521–530, 2014.

[4] K. Kushiya et al., "Development of High-Efficiency $CuIn_xGa_{1-x}Se_2$ Thin-Film Solar Cells by Selenization with Elemental Se Vapor in Vacuum," Jpn. J. Appl. Phys., vol. 34, no. Part 1, No. 1, pp. 54–60, Jan. 1995.

[5] P. Sinsermsuksakul, J. Heo, W. Noh, A. S. Hock, and R. G. Gordon, "Atomic layer deposition of tin monosulfide thin films," Adv. Energy Mater., vol. 1, no. 6, pp. 1116–1125, 2011.

[6] J. A. Andrade-Arvizu, M. Courel-Piedrahita, and O. Vigil-Galán, "SnS-based thin film solar cells: perspectives over the last 25 years," J. Mater. Sci. Mater. Electron., vol. 26, no. 7, pp. 4541–4556, 2015.

[7] T. J. Whittles, L. A. Burton, J. M. Skelton, A. Walsh, T. D. Veal, and V. R. Dhanak, "Band Alignments, Valence Bands, and Core Levels in the Tin Sulfides SnS, SnS_2, and Sn_2S_3: Experiment and Theory," Chem. Mater., vol. 28, no. 11, pp. 3718–3726, 2016.

[8] D. Nam et al., "Composition variations in $Cu_2ZnSnSe_4$ thin films analyzed by X-ray diffraction, energy dispersive X-ray spectroscopy, particle induced X-ray emission, photoluminescence, and Raman spectroscopy," Thin Solid Films, vol. 562, pp. 109–113, 2014.

[9] A. I. Oliva, R. Castro-Rodríguez, O. Solís-Canto, V. Sosa, P. Quintana, and J. L. Peña, "Comparison of properties of CdS thin films grown by two techniques," Appl. Surf. Sci., vol. 205, no. 1–4, pp. 56–64, 2003.

[10] J. Schaffner et al., "12% efficient CdTe/CdS thin film solar cells deposited by low-temperature close space sublimation," J. Appl. Phys., vol. 110, no. 6, 2011.

[11] A. Voznyi et al., "Structural and electrical properties of SnS_2 thin films," Mater. Chem. Phys., vol. 173, pp. 52–61, Apr. 2016.

[12] M. M. Ivashchenko, A. S. Opanasyuk, V. I. Perekrestov, V. V. Kosyak, Y. P. Gnatenko, and V. M. Kolomiets, "Morphological, structural, compositional properties and IR-spectroscopy of CdSe films deposited by close-spaced vacuum sublimation," Vacuum, vol. 119, pp. 81–87, 2015.

[13] V. Kosyak et al., "Composition dependence of structural and optical properties of $Cd_{1-x}Zn_xTe$ thick films obtained by the close-spaced sublimation," J. Alloys Compd., vol. 682, pp. 543–551, 2016.

[14] S. S. Hegde, A. G. Kunjomana, M. Prashantha, C. Kumar, and K. Ramesh, "Photovoltaic structures using thermally evaporated SnS and CdS thin films," Thin Solid Films, vol. 545, pp. 543–547, 2013.

[15] C. J. Panchal, A. S. Opanasyuk, V. V. Kosyak, M. S. Desai, and I. Y. Protsenko, "Structural and substructural properties of the zinc and cadmium chalcogenides thin films (a review)," J. Nano- Electron. Phys., vol. 3, no. 1 PART2, pp. 274–301, 2011.

[16] M. Devika et al., "Microstructure dependent physical properties of evaporated tin sulfide films," J. Appl. Phys., vol. 100, no. 2, 2006.

[17] K. Hartman et al., "SnS thin-films by RF sputtering at room temperature," Thin Solid Films, vol. 519, no. 21, pp. 7421–7424, 2011.

[18] P. Sinsermsuksakul et al., "Overcoming Efficiency Limitations of SnS-Based Solar Cells," Adv. Energy Mater., vol. 4, no. 15, pp. 1–7, 2014.

[19] R. Lozada-Morales, O. Zelaya-Angel, and G. Torres-Delgado, "Photoluminescence in cubic and hexagonal CdS films," Appl. Surf. Sci., vol. 175–176, pp. 562–566, 2001.

[20] O. Zelaya-Angel et al., "Raman studies in CdS thin films in the evolution from cubic to hexagonal phase," Solid State Commun., vol. 104, no. 3, pp. 161–166, 1997.

[21] D. R. T. Zahn et al., "In situ monitoring of heterostructure growth by optical spectroscopies: CdS on InP(110)," Appl. Surf. Sci., vol. 56–58, no. PART 2, pp. 684–690, 1992.

[22] [1] V. R. Minnam Reddy, S. Gedi, C. Park, R. W. Miles, and K. T. Ramakrishna Reddy, "Development of sulphurized SnS thin film solar cells," Curr. Appl. Phys., vol. 15, no. 5, pp. 588–598, May 2015.